



Abrupt Transitions and Hysteresis in Thermohaline Laboratory Models

J. A. WHITEHEAD

Department of Physical Oceanography, Woods Hole Oceanographic Institution, Woods Hole, Massachusetts

(Manuscript received 1 July 2008, in final form 5 December 2008)

ABSTRACT

As a driving parameter is slowly altered, thermohaline ocean circulation models show either a smooth evolution of a mode of flow or an abrupt transition of temperature and salinity fields from one mode to another. An abrupt transition might occur at one value or over a range of the driving parameter. The latter has hysteresis because the mode in this range depends on the history of the driving parameter. Although assorted ocean circulation models exhibit abrupt transitions, such transitions have not been directly observed in the ocean. Therefore, laboratory experiments have been conducted to seek and observe actual (physical) abrupt thermohaline transitions. An experiment closely duplicating Stommel's box model possessed abrupt transitions in temperature and salinity with distinct hysteresis. Two subsequent experiments with more latitude for internal circulation in the containers possessed abrupt transitions over a much smaller range of hysteresis. Therefore, a new experiment with even more latitude for internal circulation was designed and conducted. A large tank of constantly renewed freshwater at room temperature had a smaller cavity in the bottom heated from below with saltwater steadily pumped in. The cavity had either a salt mode, consisting of the cavity filled with heated salty water with an interface at the cavity top, or a temperature mode, in which the heat and saltwater were removed from the cavity by convection. There was no measurable hysteresis between the two modes. Possible reasons for such small hysteresis are discussed.

1. Introduction

A clear understanding of the dynamics of ocean circulation is required for many fundamental topics within earth science. For example, the contribution of ocean circulation to equator-to-pole heat flux is central to the explanation of past climate changes and is required for any prediction of future climate change. In addition, ocean circulation has fundamental consequences to biological and chemical changes within the ocean, including sequestering of CO₂. It is now well known that although over geological time the solar forcing is modified by orbital changes, the ocean surface temperature has evidently not always responded linearly. Climate records reveal occasional changes of atmospheric temperature of many degrees within "fast" times (order of 50 yr). Some of these are attributed to abrupt transitions of the thermohaline circulation regime (Broecker et al. 1985; Boyle 1990; Keigwin and Jones 1994; Keigwin et al. 1994;

Bard et al. 1996; Broecker 1997; Stocker and Wright 1991; Stocker 2000; Burns et al. 2003; Weart 2003; and many others). These findings have led to extensive modeling studies of ocean climate dynamics.

The foundation of our understanding of abrupt change for a thermohaline ocean model was established just over 50 yr ago in a simple theoretical box model of the oceans (Stommel 1961). This model had two test tanks with salt and heat diffused into the sides of the tanks from one storage tank for each test tank. One tube at the top and another at the bottom allowed circulation between the two test tanks. One storage tank containing hot salty water along with its test tank represented the tropical ocean. The other storage–test tank pair with cold and freshwater represented a polar region. The model illustrated the properties of convection with combined heat flux and freshwater flux boundary conditions. As the governing parameters (temperature and salinity differences between the two storage tanks) were slowly changed, abrupt transitions and hysteresis from one flow state to another in the test tanks were predicted by the solutions to the equations. A fuller description of a laboratory experiment that duplicates this model is given in section 2. Subsequently, abrupt transitions were

Corresponding author address: J. A. Whitehead, Department of Physical Oceanography, MS#21, Woods Hole Oceanographic Institution, Woods Hole, MA 02543.
E-mail: jwhitehead@whoi.edu

encountered in finite-amplitude stability theory for double-diffusive convection (Veronis 1965). In this example, water had a bottom boundary condition of hot salty water and a top boundary condition of cold fresh water. Below a critical value of temperature difference (or, in dimensionless terms, below the critical Rayleigh number for a wide range of diffusivity ratios, density ratios, and Prandtl numbers) the flow was stagnant, but above this value the fluid was found to be linearly unstable. However, in some parameter ranges below this critical Rayleigh number, the fluid was shown to be unstable to finite disturbances. Therefore, if the temperature difference was slowly changed, the transitions would be abrupt and there could be hysteresis.

Abrupt transitions for a numerical ocean circulation model were encountered about 30 yr ago (Bryan 1986). At that time, a number of candidates responsible for the mechanics of abrupt transition were listed as possible sources. During the next decade, abrupt jumps between thermohaline modes in numerous box model studies (summarized by Marotzke 1994 and Whitehead 1995) showed that thermohaline transitions in the ocean were primary candidates. These box model studies led to progressively more realistic ocean problems with gradually changing forcing (Rahmstorf 1995; Manabe and Stouffer 1995; Whitehead 1998; Weaver et al. 1999), with random forcing (Cessi 1994; Rahmstorf and Ganopolski 1999), and for estuarine models (Hearn and Sidhu 1999; Bulgakov and Skiba 2003). Abrupt transitions were also predicted for wind-forced convection (Stommel and Rooth 1968) and for basins forced by surface stress alone (Ierley and Sheremet 1995; Jiang et al. 1995).

Although both numerical models and data clearly indicate the possible existence of abrupt transitions in previous oceans, no temperature–salinity dataset gathered over historical time for the ocean demonstrates an abrupt transition from one type of thermohaline state to another. This includes coastal regions (estuaries, shelves, straits), despite suggestions that these would be ideal locations to find examples (Whitehead 1998; Hearn and Sidhu 1999).

The absence of physical observations of thermohaline transitions in the ocean or in any other physical system has been a primary motivation for developing laboratory studies of this important set of processes. This paper describes a sequence of laboratory experiments taken over a 10-yr period that were driven by heat and salinity flux. We initially wanted to see if abrupt transitions and hysteresis actually existed and, if so, what their features and properties would be compared to the simple models that predict them. As time went on, the studies became more refined and specific. They all produced abrupt transitions. Most of them exhibited hys-

teresis as well. The only other laboratory experiments driven by heat and salinity flux have been conducted by Bulgakov and Skiba (2003) and more recently by Mullarney et al. (2007). Both reported regime diagrams, so the transitions were abrupt, but no detailed studies of hysteresis were included.

The idea that thermal response time is smaller and thereby faster than salinity response time pervades the physics of all the numerical models mentioned above. It applies equally well to the large-scale thermohaline overturn of the oceans as well as to smaller regions such as continental shelves, estuaries, or marginal seas. It also applies to all double-diffusive problems with salt-water, because the diffusivity of salt is 10^{-2} times that of heat. Therefore, thermal response time was made to be smaller than salinity response time in all the experiments reported here. All other numerical models and laboratory experiments have also possessed this ubiquitous feature of the oceans.

This paper is inspired by all of Pedlosky's books in which the results from different studies are shown in a standard manner, so that they can readily be compared with each other. The sequence begins with a highly constrained box experiment. This first experiment (section 2) reproduced and qualitatively verified Stommel's classical box model results (Stommel 1961), showing both abrupt transitions and large hysteresis between two very different states. The second experiment (section 3) was similar to the first, but it had more "degrees of freedom" (very loosely defined) on the possible flow patterns. The transition between two flow states was abrupt, but the range of hysteresis was much smaller than the range of the first experiment. The third experiment (section 4) had a layered configuration. The data also exhibit a smaller range of hysteresis. This experiment suggested a new experimental design; the results for this new experiment are presented in section 5. In this fourth experiment, called the cavity experiment, there was no measurable hysteresis, but there still was a distinct abrupt transition. The discussion (section 6) advances a suggested mechanism for the decrease of hysteresis in the sequence of experiments.

2. The box experiment

Our initial laboratory studies to view abrupt thermohaline transitions were a modified version of Stommel's thought experiment (Stommel 1961). As described in the introduction, his original version had two well-mixed water-filled basins next to each other that were connected by tubes at the top and bottom. Heat and salt from adjacent baths diffused into each basin through sidewalls. One basin represented the tropics, with positive temperature

and salinity diffused in through a sidewall, and the other represented the poles, with negative temperature and negative salinity diffused in through the sidewalls. Because the basins were well mixed, it is irrelevant that the density changes diffuse in through the sides rather than at the tops. Our apparatus (Whitehead 1996, 1998) (Fig. 1), which we will call the box experiment here, differed somewhat from the thought experiment by having only one active basin that was connected to a large reservoir of freshwater at a fixed temperature of 20°C. The basin had saltwater pumped in with a precisely controlled flow rate at the top of a sponge. The basin was also heated from below through a copper bottom kept at a temperature $(T^*+20)^\circ\text{C}$ with the use of a thermostatic bath and pump. The heating from below and saltwater entering from above both served to mix up the water in the tank by convection. This mixing replaced the propellers in Stommel’s model. As in Stommel’s original thought experiment, because the tank was well mixed, it is irrelevant whether the boundary conditions for temperature and salinity were on the top, bottom, or sides of the test basin.

The experiment basin represents the heated test tank in Stommel’s thought experiment and thus represents the tropics, but it is in contact with a large basin of freshwater that represents a temperate ocean of lower salinity. The tubes represent the dynamics of the flow in pathways between the basin of interest and the larger ocean. The basin can also be thought of as an estuary in a desert region (or even the Mediterranean) in contact with the Atlantic Ocean. In such regions, salinity is increased by the removal of freshwater rather than the addition of saltwater, and the outer basin must have some ambient salinity rather than be fresh as in the laboratory; these alterations are easy to quantify and the governing equations are the same (Whitehead 1996). Because Stommel’s model is symmetric between the heated and cooled basins, this experiment can also be thought of as an inverted model of a polar basin that is cooled and receives freshwater. In that case, the temperature anomaly sign is reversed and the salinity value is a negative deviation from the subpolar ocean value.

The governing equations for salinity deviation S from an ambient value and temperature T above 20°C in the small basin are

$$\frac{dS}{dt} = \frac{1}{\tau_S}(S^* - S) - \frac{|Q|}{V}S, \tag{2.1}$$

$$\frac{dT}{dt} = \frac{1}{\tau_T}(T^* - T) - \frac{|Q|}{V}T, \tag{2.2}$$

where Q is the volume flux of water from the reservoir to the basin and V is the volume of the basin. The time

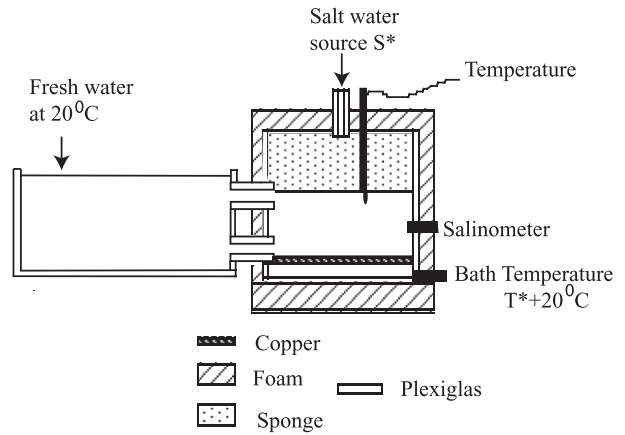


FIG. 1. The box experiment apparatus.

constants for salinity and temperature in the basin are given by $\tau_S = V/q$ and $\tau_T = \{[k/(\delta H \rho_0 C_p)] + q/V\}^{-1}$, where saltwater of salinity S^* is pumped with volume flux rate q into the top of a chamber of depth H . Note that the temperature time constant is always less than the salt time constant. The conductivity of the water is k , the reference density of the water is the density of water in the reservoir ρ_0 , and the specific heat is C_p . The boundary layer thickness δ is produced by cellular convection over the hot plate and is related to the Rayleigh number of the convection. Finally, the density of the mixed water in the chamber is taken to be a linear function of temperature and salinity:

$$\rho = \rho_0(1 + \beta S - \alpha T). \tag{2.3}$$

Equations (2.1)–(2.3) are identical to Stommel’s equations. To understand the solutions to these, he considered the steady response of (2.1), (2.2), and (2.3) to the rate of tube flux Q . (For example, imagine that a small pump drives the exchange flow between the basin and the reservoir, in one tube and out the other.) The temperature and salinity are related to flux by

$$S = \frac{S^*}{1 + \frac{|Q|\tau_S}{V}} \quad \text{and} \tag{2.4}$$

$$T = \frac{T^*}{1 + \frac{|Q|\tau_T}{V}}. \tag{2.5}$$

These describe two hyperbolas of S versus Q (one for each sign of Q) and two of T versus Q . The case with $\beta S^* > \alpha T^*$ and $\tau_S > \tau_T$ is shown in Fig. 2a. The density change from the freshwater in the reservoir is $\beta S - \alpha T$. For zero Q , the density deviation is $\beta S^* - \alpha T^*$ and positive. For the case of $\alpha T^* > \tau_T \beta S^*/\tau_S$, the density deviation changes sign as shown in the figure, and as Q becomes

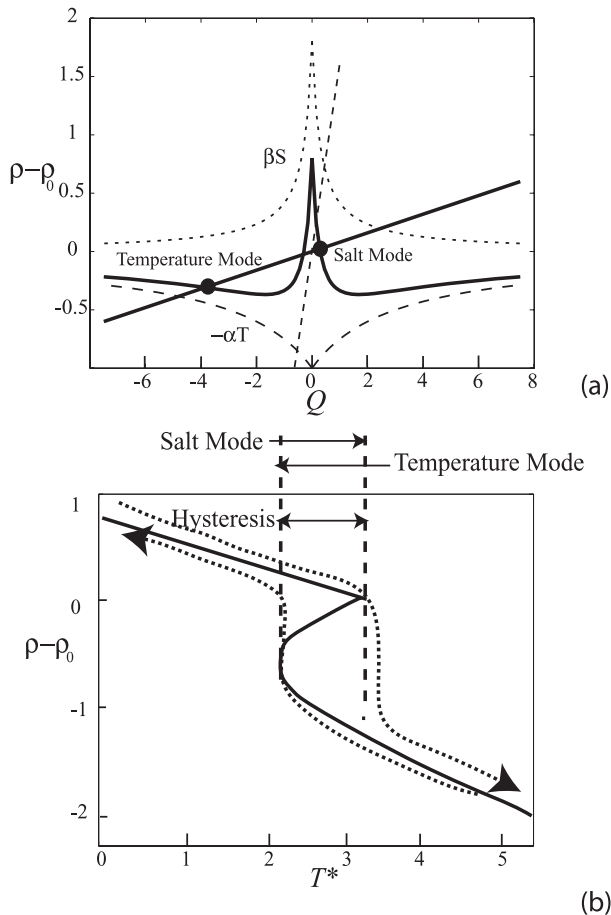


FIG. 2. (a) Curves of density deviation vs flux along with the density from salinity and temperature for parameters $\beta S^*/\alpha T^* = 1.8$ and $\tau_T/\tau_S = 0.1$. The straight lines represent the relation between buoyancy force and flow through the tubes. The S and T modes are found at intersections of density with the dark straight line. An unstable intersection point separates them. For large tube resistance, the line is very steep, and only the S mode is found. (b) The density as T^* is varied with fixed values of tube resistance constant C , pumping rate q , and salinity of the injected water S^* . The two abrupt transitions and the range of hysteresis are indicated. The dotted curves show two hysteresis trajectories.

infinite the deviation becomes zero. Thus, density can be either positive or negative depending on the value of Q . Finally, we forget about the imaginary pump and let the fluid flow through the tubes with the relation

$$Q = C(\rho - \rho_0), \quad (2.6)$$

with C being a constant that is inversely proportional to resistance of flow through the tubes. A dark straight line represents (2.6) in Fig. 2a. The solution for steady flow is an intersection between the line and the density curves. Three intersection points are shown, although for other parameters only one intersection point exists. These represent two stable fixed points (marked by solid cir-

cles and called “modes”) and one unstable one. The temperature mode has rapid flow through the tubes and salinity is very small. The salt mode has slow flow in the opposite direction, and both T and S are closer to T^* and S^* than they were in the temperature mode.

Time constants in the apparatus were measured in run-down experiments with the tubes blocked except for allowing a small outflow, with the results $\tau_S = 2000$ s and $\tau_T = 500$ s. Both numbers are only approximate because the rundown is not perfectly exponential, but it is clear that the temperature responds approximately 4 times faster than salinity. Different experimental runs had fixed values of S^* and q while T^* was varied. As T^* is increased from zero (Fig. 2b), the theory indicates that the model occupies the salt mode until the tip of a cusp is reached. Beyond that point, the model occupies the temperature mode. Conversely, when the model is already in the temperature mode and T^* is decreased, the model occupies the temperature mode until the minimum for the temperature mode is encountered, where the model reverts to the salt mode. To be internally consistent, the nomenclature we use is as follows: the jumps in density, temperature, and salinity are called “abrupt transitions.” The fact that the model has more than one mode, where the mode that is selected by the flow depends on history, is called “hysteresis.” In Fig. 2b there are two abrupt transitions and one range of hysteresis, but in more complicated models there may be more of each. Numerous studies have used other nomenclature to describe abrupt transitions and hysteresis, such as multiple equilibria, Stommel transitions, hinge points, or finite-amplitude instabilities, but we will consistently use the words *abrupt transitions* and *hysteresis*. This nomenclature is particularly useful because the ranges of both the transitions and the hysteresis can be quantified.

Note that if the flow in the tubes has sufficient resistance, only the salt mode is possible, as shown by the steep, dashed straight line in Fig. 2a. The implication for the ocean is that if the flow between two regions is sufficiently constricted, then the exchange between the two regions should be dominated by the long time-scale component of the density (the salinity). This is in fact observed for marginal basins with narrow openings such as the Mediterranean Sea, the Black Sea, Chesapeake Bay, and many estuaries, which have density fields dominated by salinity difference from the ocean rather than temperature difference. In addition, the halocline in the Arctic Ocean is dominated by salinity difference from the North Atlantic Ocean rather than temperature difference, and its presence may be due to sluggish and constricted exchange between the Arctic and North Atlantic Oceans.

Experiments were conducted using two slightly different laboratory configurations. In one configuration

(Whitehead 1996, 1998), a well-mixed chamber was connected laterally to the reservoir by two tubes one above the other. In the second configuration, the two side tubes were connected to a long channel to join the basin to the reservoir. The purpose of the channel was to help us assess the role of molecular diffusion of heat and salt in the connecting channel (Whitehead et al. 2003). In all cases, all other dimensions were identical.

Bath temperature $T^* + 20$ was regulated to 0.1°C and pumping rate q was controlled to within 0.1%. The water pumped in had a value of salinity giving $\beta S^* = 0.006$. The temperature in the basin was recorded by a thermocouple. To determine steady state, the record had to exhibit no trend in time for at least 3 h. Fluctuations from convection cells inside the basin were abundant, and they dictated the time required to be certain of steady mean temperature. Density in the basin was measured by pumping a sample into a densimeter accurate to the fifth decimal point. The pumping rate was small enough for thermal equilibrium to exist in the densimeter. From this, the salinity was determined. Then, density within the small basin was calculated using the full nonlinear equation of state for water. Therefore, we define the dimensionless density change as $\Delta\rho' = \Delta\rho/0.006$. Also, the dimensionless temperatures here and those discussed in the rest of this paper are defined as $T' = \alpha T/0.006$ and $T^{*'} = \alpha T^*/0.006$, where T is temperature in the basin in excess of 20°C .

Figure 3 presents the experimental measurements of temperature and salinity, and Fig. 4 presents dimensionless density. The data are from both configurations superimposed; there was no detectable difference. It is important to note that each point represents a complete experimental run that was conducted over a long enough time span to be convincingly steady. The initial condition for each run was not simply the run preceding it. In fact, values of T^* from one run to the next jumped around as we groped to find the range of each branch. Thus, the concept of hysteresis is true in general, but it was not specifically duplicated in this experiment. In practice, it was simple to place a flow on the T-mode branch by starting with the salinity pump off and setting the value of T^* . Then, over the course of some time the pump was brought up slowly to the steady rate. It was simple to place a flow on the S-mode branch by starting the pump first and then slowly bringing T^* up to the value. The amount of time needed to approach the final value was strongly a function of how close to the transition point one was. When one was very close, the pumping rate or temperature had to be changed slowly over the course of hours.

The data in Figs. 3 and 4 show both abrupt changes and hysteresis. Although we generally found good

qualitative agreement, the quantitative agreement with the box model theory was not exact. The value of T^* for each transition was about 20% different from theory (Whitehead et al. 2003). This is certainly due in part from a lack of precise knowledge of the time constants of the basin. In fact, the temperature time constant of the experiments was not exactly constant. Also, possibly there was small heat loss in the apparatus and perhaps mixing within the basin was not complete. Finally, the assumption of a constant value of coefficient of expansion is imperfect for water. Because of this, a linear density curve like Eq. (2.3) was not satisfactory. Note that the ocean is almost always colder than the average temperature of the experiment ($>30^\circ\text{C}$), and because colder water has relatively greater nonlinearity in the equation of state, the full equation of state is probably important for any ocean problem.

3. The slot experiment

The next experiment is called the slot experiment. It was designed to allow more freedom for vertical motion within the heated basin (Whitehead et al. 2003). A small salinity source at the top of the basin replaced the sponge. It generated less mixing. A vertical slot replaced the two tubes. A new basin was used that was slightly larger than the previous one (0.10 m high, 0.155 m wide, and 0.245 m long). It was less insulated thermally because it did not appear that a small amount of heat loss through the walls affected the behavior substantially. The walls and top were made of 0.012-m-thick Plexiglas so the flow in the basin could be viewed. As in the box experiment, it had a copper bottom in contact with water at bath temperature $T^* + 20$. Instead of two tubes, a vertical slot extended from top to bottom at one end. Although we experimented with different slot opening widths, all final experiments had a slot width of 0.01 m. The entire small basin was immersed in a large tank of freshwater at 20°C . Saltwater at the same temperature was pumped into the basin through a vertical tube extending down through a hole in the top. The elevation of the tube determined the rate of mixing of the saltwater descending to the heated copper bottom of the basin. The desire to control the rate of mixing was prompted by the fact that water-mass thickness in the ocean is intimately connected to the rate of mixing (Huang 1999) and that quantification of mixing rate in the ocean is the subject of active research (Polzin et al. 1996, 1997). Our estimate of the amount of mixing in the experiment was made using data from controlled experiments of undermixed exchange flow (Timmermans 1998). We estimate that the mixing in this experiment was less than half the rate needed for complete mixing.

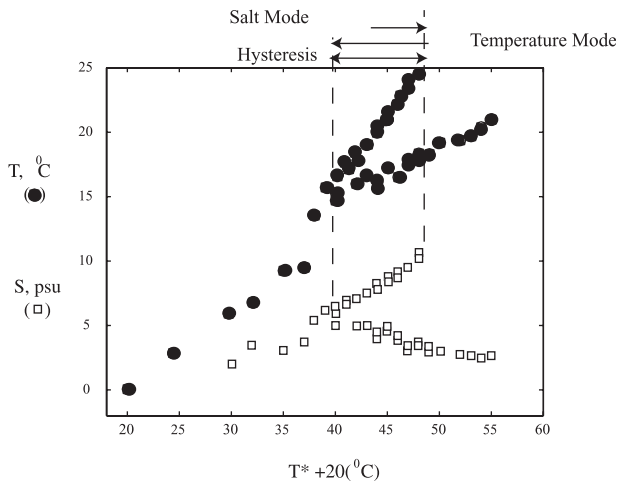


FIG. 3. Temperature and salinity in the box experiment as a function of the bath temperature.

The slot experiment was heated from below and received a steady flux of saltwater, but actually it is best thought of as an inverted model of a cooled region receiving a steady flow of freshwater at the top of a saltwater ocean. It could represent the Arctic Ocean, for example, which is cooled from above and receives a sizeable flow of freshwater from continental runoff. The fluid inside the basin could develop internal stratification and layers, and the water could enter and leave the tank at different levels. The saltwater plume descended from the top as a meandering plume and was visible through the transparent tank walls because it was dyed blue. The finite mixing from the plume can be thought to represent the low level of internal mixing in the Arctic region.

The experiments described here had as a driving parameter the bath temperature $T^* + 20$, which was varied over the maximum possible range. The tube elevation was not varied in these runs, although a second set did vary h over a limited range.

The mixture of salt- and freshwater accumulated on the copper floor, where it was heated. Then, the mixed layer left the tank in one of two different ways. The salt mode (Fig. 5) had a plume of salty water that sank to the floor of the small basin so that it covered the heated bottom. Water in the layer exited the box through the bottom region of the slot. The freshwater lying above the salty water inside the small basin was heated by conduction. Colder freshwater entered the tank at middepth, and warmer freshwater left the tank through the top of the slot.

The temperature mode (Fig. 6) had the mixed layer merge with an inflow of fresh cold water that entered in the bottom portion of the slot. The entire mixture exited as an outflow of hot salty water through the top portion.

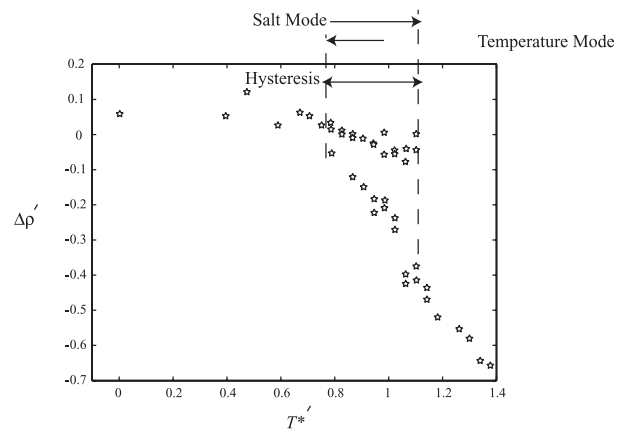


FIG. 4. Density in the box experiment as a function of dimensionless temperature of the hot bath.

The water in the interior of the chamber appeared to have more of a uniform color. Therefore, we assume from the photographs that the salinity is more uniform and that it was not as layered as it was in the salt mode. An arrested salt wedge was usually seen along the floor of the chamber. It had very strong mixing at the nose. However, detailed measurements of all the mixing within the basin were not obtained.

Each experiment was conducted for many hours to convince us that equilibrium had been reached. There was no intermediate type of flow between the two modes, and the transition from one to the other was abrupt. This is quantified by measurement of the density of samples at the bottom of the tank in the corner away from the slot (Fig. 7). The dimensionless density salinity has the definition $S' = (\rho - 998.2)/(\rho^* - 998.2)$ with density measured by a sample pumped into the laboratory densimeter and brought to 20°C . This showed a clear jump in S' near the value $T^* \approx 0.5$. Time series of temperature were unfortunately not measured. Density samples were taken at many other locations too, but this location proved to be the most reliable because there was no interface moving up and down nor sinking plume to introduce positive or negative salinity fluctuations. The range of hysteresis was easy to verify, because in that range it was possible to switch artificially from one flow to another. For example, if the flow was in the salt mode and we inserted a rod through the slot and mixed, this triggered a switch to the temperature mode within 30 min, which permanently remained (as long as the experiment was continued with that value of T^*). In contrast, decreasing mixing by lowering the elevation of the source when the flow was in the temperature mode resulted in the flow switching to the salt mode, which would permanently remain after the source was returned to the original elevation.

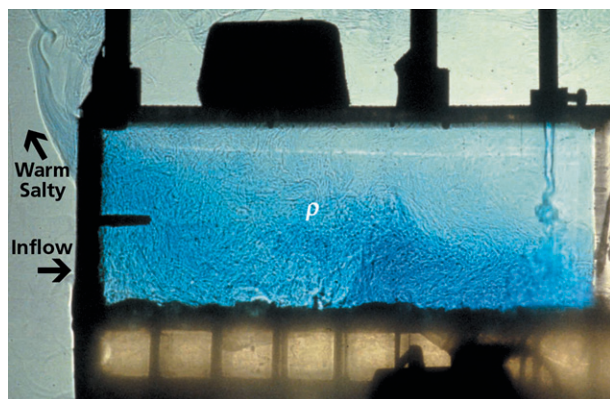


FIG. 5. Side view of the salt mode in the slot experiment.

In summary, this experiment was designed to allow more latitude for flow structures to exist than the over-mixed box model and did fulfill that requirement. Two principal differences were found. First, the salt mode was composed of three layers and the temperature mode only two. Second, the range of hysteresis was smaller than in the box experiment.

The three-layered salt mode has the vertical characteristics of the exchange between the Arctic and North Atlantic. Thus, cold freshwater flows out of the Arctic regions along the coast of Greenland and through the Canadian islands, while cold salty water spills over the Denmark and Fram Straits. Warmer salty water flows into the Norwegian Sea in the North Atlantic Current.

4. The layered experiment

It was found (Whitehead 2000) that a layer of freshwater lying over salty water serves the same dynamical purpose as the pumped saltwater in the previous two experiments. The ocean itself suggested this, because in polar oceans a surface layer that is 100–300 m deep of lower-salinity water acts as a “cooling barrier” to deep convection. Polar oceans lack widespread deep penetration of dense, newly chilled surface water (deep convection) during winter, except for extraordinarily cold winters. These abrupt sinking events are very important for causing cold salty water ($<2^{\circ}\text{C}$, >35 psu) of polar origin to sink and fill all oceans below about 2000 m. The required volume flux is large, on order $10^7 \text{ m}^3 \text{ s}^{-1}$. Wintertime deep convection examples are known in the Labrador Sea, in the Greenland Sea, within the Gulf of Lyons in the western Mediterranean Sea, and in the Weddell Sea. In addition, sea-ice growth is strongly retarded in the Arctic when the freshwater layer is not present (Björk et al. 2002) and when events characterized by changes in layer salinity of the Arctic Ocean freshwater layer are known (Swift et al. 2005). These could all produce effects on

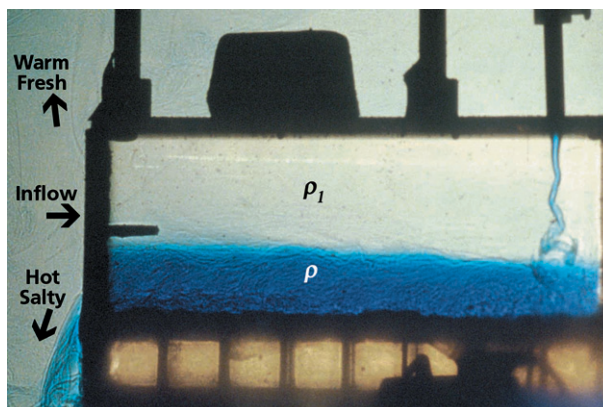


FIG. 6. Side view of the temperature mode in the slot experiment.

the large global climate cycles (Broecker et al. 1985; Boyle 1990; Keigwin and Jones 1994; Keigwin et al. 1994; Broecker 1997; Burns et al. 2003).

This experiment (Whitehead et al. 2005; Whitehead and Bradley 2006) was designed to test a theory for layered convection (Whitehead 2000) that predicted abrupt transitions and hysteresis. A layer of freshwater above saltwater is cooled from above in one basin. A second basin next to it contains the layer above saltwater, with both at the same fixed temperature. If the water in the cooled basin becomes denser, the layer becomes deeper and water from the fixed basin flows in through a tube connecting them at the surface. There are two additional tubes connecting the basins, one at mid-depth and one at the bottom of the deep layer. Because this experiment is cooled rather than heated, it is equivalent to the polar basin in Stommel's original experiment. Therefore, the salt mode involves lower salinity water here. The salt mode in this experiment has fresh surface water slowly drawn into the small basin through the top tube and cooled. It achieves cold temperatures and leaves the small basin through the lower tubes. The water remains fresh because no saltwater flows into the small basin. We call it a salt mode because the convecting water has different salinity from the deep water in the large basin (which represents the saltwater of the deep ocean). The temperature mode flows more rapidly. Flow in the middle tube reverses direction compared to the fresh mode so that rapid inflow of middepth saltwater from the large basin mixes in the small basin, with freshwater entering through the top tube, and the cold mixture exits through the bottom tube. Theory shows that it is necessary to have the top tube more constricted than the two others to produce the flow reversal in the middle tube. It is this flow reversal that leads to abrupt transitions and hysteresis as T^* is changed.

The layer of freshwater can be thought of as the surface layer of lower salinity water that is present in all

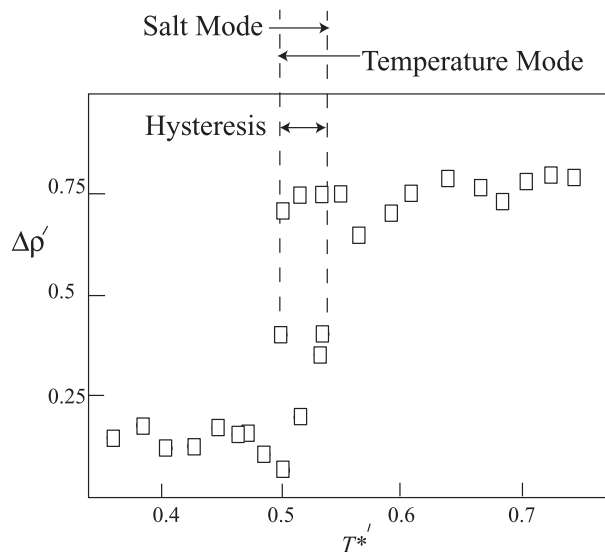


FIG. 7. Values of density of a sample taken from the right-hand end at the bottom of the basin in the slot experiment.

polar seas. The top tube represented the flow pathway for additional freshwater to enter the cooled region. The middle tube represented the pathway for flow between the deep mixed layer in a polar ocean during wintertime convection and the saltier water at middepth next to it. The bottom tube represented the pathway for removing the densest water from the region of deep wintertime convection.

The laboratory experiment to test this had a cooled smaller basin next to a larger tank along with three tubes just like the thought experiment (Fig. 8). The larger tank on the right received an inflow of freshwater at the top, an inflow of saltwater at the bottom (both through sponges to minimize turbulent mixing), and an outflow through a hole in the sidewall at 2.5 cm below the water surface. The outflow water ascended within an exit tube to an overflow and spilled over it into a drain. In this way, the interface of the fresh surface layer was kept at a fixed elevation, and the submerged exit maintained a sharp interface between fresh- and saltwater. A heat exchanger in the large basin maintained the large basin temperature steadily at 20°C within acceptable limits.

The smaller basin on the left was the dynamically active component of the experiment. It was cooled from above with a copper container filled with chilled water at temperature $T^* + 20$ (T^* is a negative number). Because the fresh surface layer is cooled from above, the mixed layer deepens from cooling. An inflow of freshwater through the top tube from the right-hand basin to the left introduces additional freshwater in response to the cooling and deepening of the layer. It was shown in the

linear theory that flow reversal in the middle tube and hence abrupt transitions are only encountered if the resistance to flow of the top fluid is greater than the resistance of the other tubes. Therefore, the top tube contained an insert with a very small diameter tube. The resistance of the tube was calibrated by blocking the tube, removing the surface layer in the small basin by suction so the test basin was filled with saltwater, then removing the block and letting a surface layer drain into the test small basin while timing the thickening of the layer in the small basin (all at $T^* = 0$). The resistance is of order 10^{-4} times the resistance of the large tube.

The intensity of the thermal driving is measured by the dimensionless number $T^{*'} = -\alpha T^*/\beta S_0$, where $-\alpha T^*$ is the maximum possible density increase from cooling (because $T^* < 0$), and βS_0 is the density difference between the fresh- and saltwater. This is the driving parameter in the experiments and is held at a constant value in the range $0.5 < T^{*'} < 1$ for each run. Another dimensionless number is the tube resistance ratio γ , defined as the top tube flow resistance divided by lower tube flow resistance. The theory shows that for $\gamma < 0.5$, as $T^{*'}$ is gradually increased, there is a sudden increase of layer salinity S because saltwater is entering that layer through the middle tube and mixing into it. Concurrently, the heat flux out of the top layer increases. This is accompanied by an increase in mixed layer temperature T as the salt mode, characterized by very cold water, jumps to the warmer temperature mode. As $T^{*'}$ becomes less again, there is a jump back to the salt mode at a second value. Conversely, for $\gamma \geq 0.5$ multiple equilibria are not found. For our laboratory apparatus, γ is of order 10^{-4} . For practical purposes, this means that the lower half of the small basin has active circulation with the large basin through the two bottom tubes. Therefore, the salty water in the small basin below the freshwater layer has ambient salinity and temperature.

Four different flow regimes were found. Three regimes have steady flow and the fourth is cyclic in time with periods greater than 1 h.

Regime 1 (sketched in Fig. 9a) has exchange flow in the middle tube and is therefore not in the theory encompassed by Whitehead (2000), which assumed unidirectional tube flow. The interface in the small basin is located below the midplane of the middle tube, and there is an interface between dyed and clear fluids within the middle tube.

Regime 2 has a steady flow (Fig. 9b) and corresponds most closely to the salt mode of the theory. This mode is indicated by the presence of only dyed freshwater in the middle tube flowing out of the small basin. The interface between fresh- and saltwater has reached the bottom of the small basin in this regime, and dyed freshwater flows

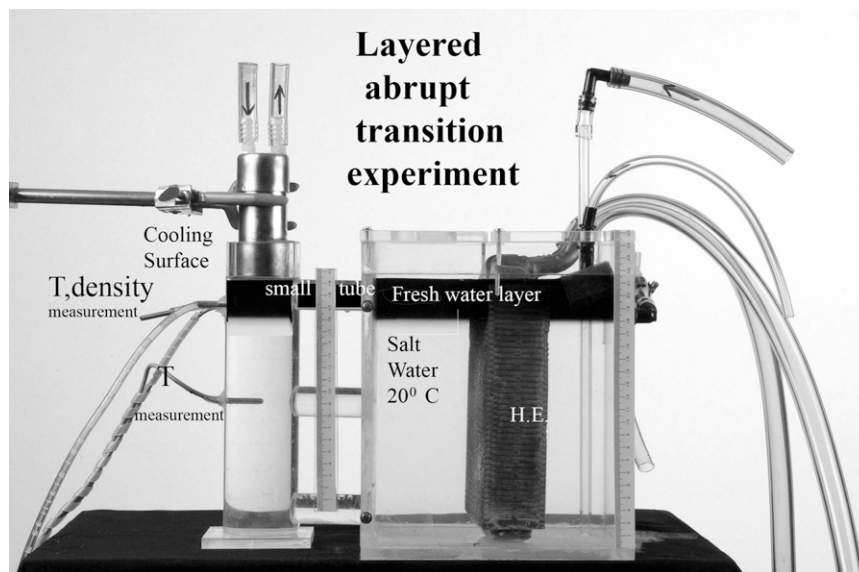


FIG. 8. Apparatus for the layered experiment.

out of the small basin through the bottom tube as well as the middle tube. As a consequence, the water in the small basin is completely fresh, and because it is well mixed by cooling from above, the dye is relatively uniform everywhere.

Regime 3 (Fig. 9c) corresponds most closely to the temperature mode. Clear salty water rapidly enters the small basin through the middle tube and ascends to the top. (In the theoretical model, flow reversal only happens if the cold water in the small basin is denser than the deep saltwater in the outer tank. Therefore, the model predicts that the inflowing saltwater would be lighter than the water in the small basin, and the rising clear salty water in the experiment verifies this prediction.) It gets cooled there and turbulently mixes with a very small amount of dyed freshwater that flows in through the top tube. The cooled mixture descends top to bottom in the small basin as cold convection, and the cold mixture leaves through the bottom tube.

Regime 4 has time-dependent flow (Whitehead et al. 2005). This regime is described here but is not the topic of this study, so details and supporting theory are not included. As the layer of dyed freshwater is cooled in the small basin, the depth of the layer slowly increases and the color intensity decreases by a small amount. Suddenly a new dyed layer forms at the top. At the base of this new layer is a new internal interface that begins to move downward just like the movement of the first interface. Below this new interface, the color intensity of the old layer fades dramatically, and finally the old layer mixes together with the water below it. For all practical purposes, this means that the old layer van-

ishes. This cyclic behavior is dominated by changes in salinity in the layers with time, and for all practical purposes, the flow is in the salt mode during the cycle. A similar oscillation is observed in the experiment by Mullarney et al. 2007, but the apparatus has a closed tank with a heater on one end of the bottom, cold temperature at the other end, and saltwater injected at the heated end. Thus, it is closer to the slot experiment.

The experimental results show that there is a small range of hysteresis between the salt mode and the temperature mode (Fig. 10). The salt mode existed for smaller values of driving temperature, although oscillations occurred in some of the data points (shown with bars). There was a rough qualitative agreement between the theory and data, but quantitative comparison was only good to within a factor of 2 or so. The data do not track the theoretical curves very closely, but that is to be expected because there was heat leakage in the apparatus and also mixing in the interface at the bottom of a layer is not contained in the theory. In addition, the resistance coefficient of the tube was only roughly quantified, and the exchange rate between the surface cooling and the water was only roughly quantified. Finally, the temperature range was 4°–20°C so that the nonlinear equation of state for water is needed and the coefficient of expansion varies greatly with temperature.

5. The cavity experiment

After completing the experiments described in the preceding sections, it seemed likely that an even simpler laboratory arrangement might also show abrupt

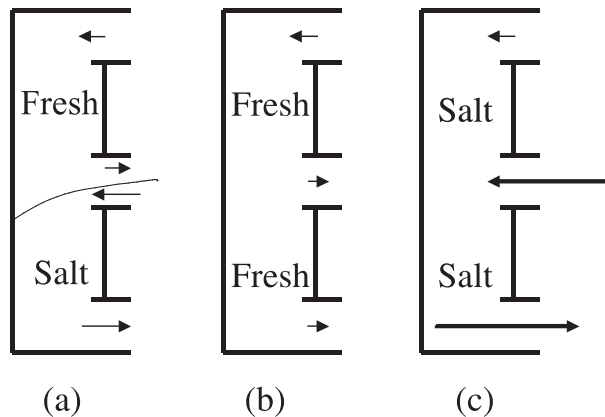


FIG. 9. Sketch of the flows for the three steady modes in the layered experiment. (a) Convection in each water layer with interface in the middle tube (regime 1); (b) the salt mode (regime 2); (c) the temperature mode (regime 3).

transitions, hysteresis, or oscillations. A hint of how to design such an experiment came from the preceding experiment in section 4 and associated theory of Whitehead et al. (2005) that showed that some of the oscillations involving the salty layer migrated up and down between the bottom and the middle tubes without reaching the middle tube. Thus the oscillations may not be due entirely to the three-tube arrangement. This motivated new experiments in which the basin to the left in the three-tube experiment was duplicated but the rest of the apparatus was removed. In addition, we reverted to having the basin heated from below rather than cooled from above. This resulted in a range of temperatures from 20° to 40°C in which the nonlinear aspects of water's equation of state are smaller. Also, the basin received a steady flux of saltwater pumped in through a tube at a constant rate. Finally, a large tank filled with freshwater was located above this basin, replacing all the tubes and the layered large container. The apparatus is called the cavity experiment (Fig. 11). In the apparatus a cylindrical cavity that was $d_c = 6$ cm deep and had a radius $r = 2.5$ cm was located in the bottom of a larger 35 cm \times 35 cm \times 40 cm tank that was flushed with freshwater maintained at a steady temperature of 20°C. The temperatures in the cavity and in the large basin were continuously measured. The rim of the cavity was elevated 1 cm above the floor of the large tank so that if the cavity became filled with salty water, the saltwater could spill over the rim into the deeper floor of the large basin and then be swept away by the circulation in the large tank. The bottom of the cavity was a 0.63-cm-thick copper plate below which water of temperature $T^* + 20$ was flushed from a thermostatic bath. Therefore, the water in the cavity was heated from below. The cavity also received a steady flow of dense saltwater of salinity S^* pumped at steady

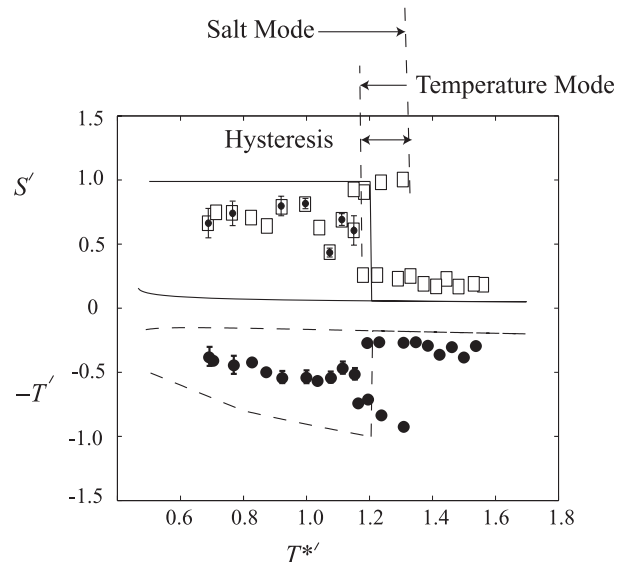


FIG. 10. Dimensionless temperature and salinity for the layered experiment. The lines and curves are from theory.

volume flux Q from a tube that extended from above into the cavity. The tube end was adjustable so that it could be elevated a distance h above the cavity bottom.

Temperature was measured by a probe accurate to 0.1°C that was fixed about 0.01 m above the copper bottom. This distance was judged to be great enough to be located above any thermal convection boundary layer, and it was intended to measure temperature in the interior of a mixed region. Typical records revealed abundant evidence of convection thermals rising from the hot bottom. Salinity was measured with a density meter using water slowly pumped from the bottom of the cavity. The water was heated to 20°C by this device and then returned to the chamber.

The cavity experiment is heated from below and receives a steady flux of saltwater. Like the slot experiment, it is probably most relevant to the inverted case of cooling of a steady flow of freshwater at the top of a saltwater ocean. It could represent the Arctic Ocean, for example, which is cooled from above and receives a sizeable flow of freshwater from continental runoff. The cavity itself was confined laterally to prevent spreading out of the layer of salty water. In the same way, the layer of freshwater that leaves the Arctic Ocean is confined to narrow boundary currents along the Greenland coast and by shallows and islands in the Canadian archipelago. The mixing between the saltwater layer in the cavity and the overlying freshwater has a counterpart in the Arctic Ocean. Freshwater of the halocline mixes down into the salty water of Atlantic origin. In both cases, double diffusion (the inverse of the salt finger case) obviously

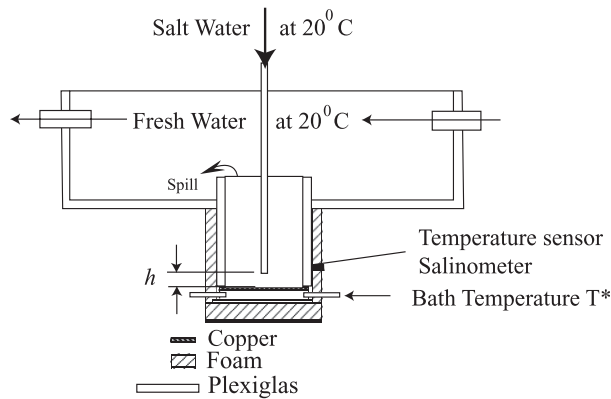


FIG. 11. The cavity experiment.

plays a role in the heat and salt flux budget, although the quantitative rates are not quantified yet.

The flow in this cavity exhibited two distinct flows that corresponded to the temperature mode and the salt mode in the previous experiments. The salt mode was dominated by dense saltwater that filled the cavity. Upwelling of the saltwater from the floor of the cavity was slow, and the dense heated saltwater rose to the top of the cavity and spilled out into the large tank where it was dispersed by the large flushing motion of the water in this tank. There was a significant interface between saltwater that emerged from the cavity and the freshwater in the large basin. Double-diffusive transport of heat and salinity was visible at this interface (as plumes of salty water rising above the layer and plumes of freshwater sinking below the layer—the salinity revealed by food coloring dye in video and still images). This exchange of heat and salt served the same dynamical purpose as the transport by advection through two tubes used in section 2 and the slot used in section 3. We also noted for the experiment in section 4 that double diffusion was probably exchanging heat and salt in the base of the layers in the layered experiments.

In contrast, the temperature mode had freshwater occupying the cavity that was mixed with a tiny amount of salty water within the cavity. The flow rate from thermal convection due to heating the bottom of the cavity was great enough to mix the saltwater from the pump up and out of the cavity. There was no significant interface between the fluid in the cavity and the fluid in the basin above.

Dynamic variables for this cavity were the density difference between the salt- and freshwater $\beta S^* = 0.006\ 00$; the rate of flow of the saltwater into the cavity, which was $q = 0.010\ \text{cc s}^{-1}$; the elevation of the tube end above the cavity bottom h ; and the temperature of the heated bath that supplied water below the copper plate $T^* + 20$. The values of salinity flow rate of the pumped water and the

tube tip elevation h were all kept fixed at the given values. The value of T^* was varied from run to run. After we found that hysteresis was almost completely absent, a number of runs were made with fixed T^* and h varied, and we found that hysteresis was also absent. This second set of runs was only conducted over a small range of h so the dataset was not very complete, and only the data for the first set of runs with variation of T^* are shown here.

The measured properties were the temperature from a probe and density of water pumped into the densimeter. Both measurements were recorded continuously to yield a time series. The final values reported were averages collected over at least 1 h. The runs themselves took at least 3 h, and runs close to the transition took even longer. The measured variables are given as the ordinates in Fig. 12. Density was measured directly with a densimeter and subtracted from freshwater density; the result was divided by $\beta S = 0.0060$. Temperature was multiplied by the nominal coefficient of thermal expansion of 2×10^{-4} , which is the value for pure water at about 20°C , and then divided by 0.0060. The abscissa shows the strength of the scaled temperature forcing.

Initial conditions were varied in numerous runs, but such variations did not affect the final states. For example, some runs were started by turning on the pump first. The bath temperature $T^* + 20$ was set to the desired value a few minutes later. Therefore, the cavity was initially filled with salty water. In other cases, the runs were started by setting the bath temperature first. Therefore, the cavity was filled with freshwater heated from below. Then the salt pump was started. Others were started by the change of one parameter from a previous run. In all cases, the final flow was found to be independent of this history.

Because the actual coefficient of expansion changes with mean temperature, it is more accurate to calculate density using the full equation of state for seawater at atmospheric pressure. It was important to estimate the density of the overhead water, thus the temperature and salinity of the overhead water were also measured as a long time series and the density determined. The densimeter values of the cavity water were used to calculate salinity; then those values of salinity were used along with the temperature measurements to calculate density of the cavity water. The results (Fig. 13) show that the density difference between the cavity water and the ambient water gradually became smaller as T^* was increased but that the abrupt transition was still distinct. In addition, the dimensionless density difference as the transition was approached from below is not zero, but it is about the value 0.1, so the interface did not simply approach neutral density difference and then mix. Instead, a stability criterion of the interface was reached at

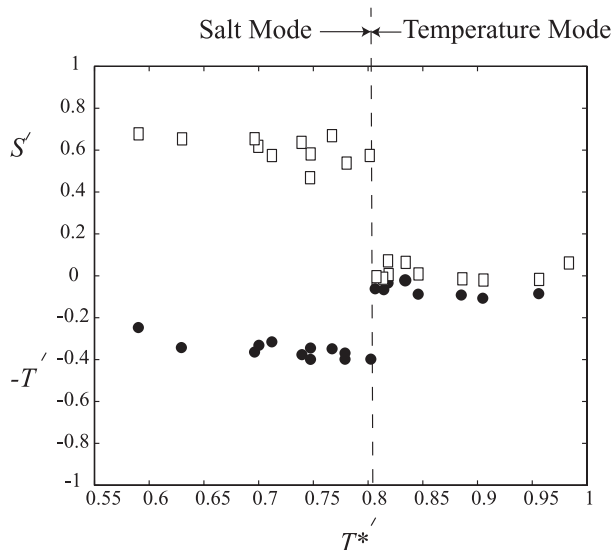


FIG. 12. Dimensionless temperature and salinity in the cavity experiment.

transition. Beyond this, the interface became unstable and the cavity water mixed with the ambient water.

The instability and overturning during transition took over an hour to be completed, but it was very simple to see with time-lapse video. It consisted of slowly growing interfacial waves with a wave period on the order of a few minutes. The impression is that the growing waves are slow enough so that the crests and troughs change temperature. These steep waves turned over, broke, and led to the complete mixing of water in the cavity. Each breaking wave seemed to decrease the salinity of the cavity water and thus drove it toward neutral density, until finally the cavity water was completely mixed. The entire time for the cavity to become unstable and mix was over an hour. The quality of frames grabbed from the video is very poor and not of sufficient quality to be given here, unfortunately. The interfacial instability seems to be a finite-amplitude counterpart of the growing oscillatory instability originally calculated by Veronis (1965) for convection in a layer bounded above and below.

The experiment was therefore a very precise method to approach the range where the density ratio approaches 1. We hope to produce a refined experiment that will give even more precise measurements of the instability and transition, and allow detailed measurement of the flux of both temperature and salinity in the range with density ratio close to 1.

6. Summary and discussion

The range of hysteresis appears to decrease as the experiments allow more possible modes of flow in the exchange region between basins and more modes of

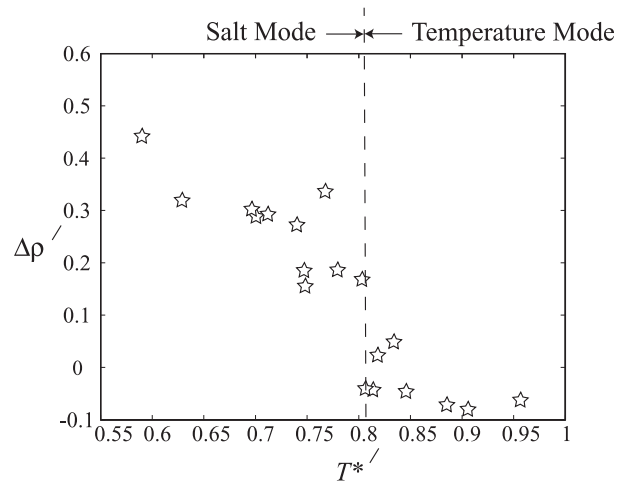


FIG. 13. Dimensionless density difference between the cavity and the overlying water in the cavity experiment.

stratification in the interior. Both can be loosely regarded as giving progressively more degrees of freedom as we proceed through the experiments sequentially from section 2 to section 5. The results seem to be consistent with some tendencies found in the calculations of simple Stommel box models with stochastic salt forcing (Stommel and Young 1993; Cessi 1994). They show, within a range of certain specific parameters, how the solution moves around within its stable potential well from random forcing and how the flow jumps from one well to the other. Although they presented no quantified measure of hysteresis, it seems logical that hysteresis would be decreased by such a process. It is useful to picture the effect of noise on a system with two potential wells in which the relative depth of the two wells is gradually changing as a control parameter is changed. If such a system is close to an end point, one of the two potential wells is very shallow. In that case, any random forcing from noise might be large enough to expel the flow from the shallow well quite effectively. In contrast, the other well would be deep enough to completely trap the flow in that state. This would mean that the solution would be expelled from the shallow well most of the time, but rarely expelled from the deep well (a result well known for tuning FM radios). This might result in a smaller range of hysteresis.

The cavity experiment is beginning to show us the link between these abrupt changes driven by mixed boundary conditions (starting with the Stommel thought experiment, 1961) and the more thoroughly studied double-diffusion processes (Turner 1973; Schmitt 1994). We anticipate that both processes will be linked more clearly in the future. Experiments with mixed boundary conditions and double diffusion should help form a more complete understanding of two-component fluid mechanics.

Acknowledgments. Support is gratefully acknowledged from the Woods Hole Oceanographic Institution Climate Change Institute, the National Science Foundation, Physical Oceanography Section under Grant OCE-0081179, and the Paul M. Fye Chair of the Woods Hole Oceanographic Institution.

REFERENCES

- Bard, E., B. Hamelin, M. Arnold, L. Montaggioni, G. Cabioch, G. Faure, and F. Rougerie, 1996: Deglacial sea-level record from Tahiti corals and the timing of global meltwater discharge. *Nature*, **382**, 241–244.
- Björk, G., J. Söderkvist, P. Winsor, A. Nikolopoulos, and M. Steele, 2002: Return of the cold halocline layer to the Amundsen Basin of the Arctic Ocean: Implications for the sea ice mass balance. *Geophys. Res. Lett.*, **29**, 1513, doi:10.1029/2001GL014157.
- Boyle, E. A., 1990: Quaternary deepwater paleoceanography. *Science*, **249**, 863–870.
- Broecker, W. S., 1997: Thermohaline circulation, the Achilles heel of our climate system: Will man-made CO₂ upset the current balance? *Science*, **278**, 1582–1588.
- , D. M. Peteet, and D. Rind, 1985: Does the ocean atmosphere system have more than one stable mode of operation? *Nature*, **315**, 21–26.
- Bryan, F., 1986: High-latitude salinity effects and interhemispheric thermohaline circulations. *Nature*, **323**, 301–304.
- Bulgakov, S. N., and Y. N. Skiba, 2003: Are transitions abrupt in Stommel's thermohaline box model? *Atmosfera*, **16**, 205–229.
- Burns, S. J., D. Fleitmann, A. Matter, J. Kramers, and A. A. Al-Subbary, 2003: Indian Ocean climate and an absolute chronology over Dansgaard/Oeschger events 9 and 13. *Science*, **201**, 1365–1367.
- Cessi, P., 1994: A simple box model of stochastically forced thermohaline flow. *J. Phys. Oceanogr.*, **24**, 1911–1920.
- Hearn, C. J., and H. S. Sidhu, 1999: The Stommel model of shallow coastal basins. *Proc. Roy. Soc. London*, **A455**, 3997–4011.
- Huang, R. X., 1999: Mixing and energetics of the oceanic thermocline circulation. *J. Phys. Oceanogr.*, **29**, 727–746.
- Ierley, G. R., and V. A. Sheremet, 1995: Multiple solutions and advection-dominated flows in the wind-driven circulation. Part 1: Slip. *J. Mar. Res.*, **53**, 703–733.
- Jiang, S., F.-F. Jin, and M. Ghil, 1995: Multiple equilibria, periodic, and aperiodic solutions in a wind-driven, double-gyre, shallow-water model. *J. Phys. Oceanogr.*, **25**, 764–786.
- Keigwin, L. D., and G. A. Jones, 1994: Western North Atlantic evidence for millennial-scale changes in ocean circulation and climate. *J. Geophys. Res.*, **99**, 12 397–12 410.
- , W. B. Curry, S. J. Lehman, and S. Johnsen, 1994: The role of the deep-ocean in North Atlantic climate change between 70-Kyr and 130-Kyr ago. *Nature*, **371**, 323–326.
- Manabe, S., and R. J. Stouffer, 1995: Simulation of abrupt climate change induced by freshwater input to the North Atlantic Ocean. *Nature*, **378**, 165–167.
- Marotzke, J., 1994: Ocean models in climate problems. *Ocean Processes in Climate Dynamics: Global and Mediterranean Examples*, P. Malanotte-Rizzole and A. R. Robinson, Eds., Kluwer Academic, 79–109.
- Mullarney, J., R. W. Griffiths, and G. O. Hughes, 2007: The role of freshwater fluxes in the thermohaline circulation: Insights from a laboratory analogue. *Deep-Sea Res. I*, **54**, 1–21.
- Polzin, K. L., K. G. Speer, J. M. Toole, and R. W. Schmitt, 1996: Intense mixing of Antarctic Bottom Water in the Equatorial Atlantic Ocean. *Nature*, **380**, 54–57.
- , J. M. Toole, J. R. Ledwell, and R. W. Schmitt, 1997: Spatial variability of turbulent mixing in the abyssal ocean. *Science*, **276**, 93–96.
- Rahmstorf, S., 1995: Bifurcations of the Atlantic thermohaline circulation in response to changes in the hydrological cycle. *Nature*, **378**, 145–149.
- , and A. Ganopolski, 1999: A simple theoretical model may explain apparent climate instability. *J. Climate*, **12**, 1349–1352.
- Schmitt, R. W., 1994: Double-diffusion in oceanography. *Annu. Rev. Fluid Mech.*, **26**, 255–285.
- Stocker, T. F., 2000: Past and future reorganizations of the climate system. *Quat. Sci. Rev.*, **19**, 301–319.
- , and D. G. Wright, 1991: Rapid transitions of the ocean's deep circulation induced by changes in surface water fluxes. *Nature*, **351**, 729–732.
- Stommel, H., 1961: Thermohaline convection with two stable regimes of flow. *Tellus*, **3**, 224–230.
- , and C. Rooth, 1968: On the interaction of gravitational and dynamic forcing in simple circulation models. *Deep-Sea Res.*, **15**, 165–170.
- , and W. R. Young, 1993: The average T–S relation of a stochastically forced box model. *J. Phys. Oceanogr.*, **23**, 151–158.
- Swift, J. H., K. Aagaard, L. Timokhov, and E. G. Nikiforov, 2005: Long-term variability of Arctic Ocean waters: Evidence from a reanalysis of the EWG data set. *J. Geophys. Res.*, **110**, C03012, doi:10.1029/2004JC002312.
- Timmermans, M. L. E., 1998: Hydraulic control and mixing in a semi-enclosed reservoir. Geophysical Fluid Dynamics Summer Study Program Tech. Rep. WHOI-98-09, 175–190.
- Turner, J. S., 1973: *Buoyancy Effects in Fluids*. Cambridge University Press, 367 pp.
- Veronis, G., 1965: On finite amplitude instability in thermohaline convection. *J. Mar. Res.*, **23**, 1–17.
- Weart, S., 2003: The discovery of Rapid Climate Change. *Phys. Today*, **56**, 30–36.
- Weaver, A. J., C. M. Bitz, A. F. Fanning, and M. M. Holland, 1999: Thermohaline circulation: High-latitude phenomena and the difference between the Pacific and Atlantic. *Annu. Rev. Earth Planet. Sci.*, **27**, 231.
- Whitehead, J. A., 1995: Thermohaline ocean processes and models. *Annu. Rev. Fluid Mech.*, **27**, 89–114.
- , 1996: Multiple states in doubly-driven flow. *Physica D*, **97**, 311–321.
- , 1998: Multiple T–S states for estuaries, shelves and marginal seas. *Estuaries*, **21**, 278–290.
- , 2000: Stratified convection with multiple states. *Ocean Modell.*, **2**, 109–121.
- , and K. Bradley, 2006: Laboratory studies of stratified convection with multiple states. *Ocean Modell.*, **11**, 333–346.
- , M. L. E. Timmermans, W. G. Lawson, S. N. Bulgakov, A. M. Zatarian, J. F. A. Medina, and J. Salzig, 2003: Laboratory studies of thermally and/or salinity-driven flows with partial mixing. Part 1: Stommel transitions and multiple flow states. *J. Geophys. Res.*, **108**, 3036, doi:10.1029/2001JC000902.
- , L. te Raa, T. Tozuka, J. B. Keller, and K. Bradley, 2005: Laboratory observations and simple models of slow oscillations in cooled salt-stratified bodies. *Tellus*, **57A**, 778–809.